Forensic Science International 298 (2019) 323–331

Contents lists available at ScienceDirect

Forensic Science International

journal homepage: www.elsevier.com/locate/forsciint

Determining the region of origin of blood spatter patterns considering fluid dynamics and statistical uncertainties

Daniel Attinger[a,*], Patrick M. Comiskey[b], Alexander L. Yarin[b], Kris De Brabanter[c,d]

[a] Mechanical Engineering, Iowa State University, 50010 Ames, IA, USA
[b] Department of Mechanical and Industrial Engineering, University of Illinois at Chicago, 842 W Taylor St., Chicago, IL 60607-7022, USA
[c] Department of Statistics, Iowa State University, 50010 Ames, IA, USA
[d] Department of Computer Science, Iowa State University, 50010 Ames, IA, USA

ARTICLE INFO

Article history:
Received 24 September 2018
Received in revised form 23 January 2019
Accepted 5 February 2019
Available online 15 February 2019

Keywords:
Bloodstain pattern analysis
Ballistic
Reconstruction
Fluid dynamics
Probabilities
Uncertainty propagation

ABSTRACT

Trajectory reconstruction in bloodstain pattern analysis is currently performed by assuming that blood drop trajectories are straight along directions inferred from stain inspection. Recently, several attempts have been made at reconstructing ballistic trajectories backwards, considering the effects of gravity and drag forces. Here, we propose a method to reconstruct the region of origin of impact blood spatter patterns that considers fluid dynamics and statistical uncertainties. The fluid dynamics relies on defining for each stain a range of physically possible trajectories, based on known physics of how drops deform, both in flight and upon slanted impact. Statistical uncertainties are estimated and propagated along the calculations, and a probabilistic approach is used to determine the region of origin as a volume most compatible with the backward trajectories. A publicly available data set of impact spatter patterns on a vertical wall with various impactor velocities and distances to target is used to test the model and evaluate its robustness, precision, and accuracy. Results show that the proposed method allows reconstruction of bloodletting events with distances between the wall and blood source larger than ~1 m. The uncertainty of the method is determined, and its dependency on the distance between the blood source and the wall is characterized. Causes of error and uncertainty are discussed. The proposed method allows the consideration of stains indicating impact velocities that point downwards, which are typically not used for determining the height of the origin. Based on the proposed method, two practical recommendations on crime scene documentation are drawn.

1. Introduction

Bloodstain Pattern Analysis (BPA) is one of many techniques of forensic science and crime scene investigation [1,2]. Besides the determination of the mechanisms causing specific collections of stains (patterns), BPA also aims at reconstructing *blood spatter patterns* — patterns generated by impact of airborne drops on a target surface. For spatter patterns, the determination of the 3D location of the spatter producing event – *the region of origin* – is relevant to criminal cases. Note that the term *region of origin* used throughout the manuscript departs from current standards [3] in BPA, which recommend *area of origin*. We find that term confusing because of its 2D technical meaning, while the origin of a spatter is clearly a 3D region of space which the work in this manuscript identifies and measure as a volume. As translated from the 1939 extensive and seminal BPA study of Balthazard et al., "*The problem of reconstructing curved trajectories is very difficult to solve*" [4]. Indeed, proper backward reconstruction of the trajectory of a single drop relies on the determination of the three impact velocity components, as well as the drop volume, the latter necessary for the consideration of drag forces along the trajectory.

Backward trajectory reconstruction typically involves the following steps: (1) the inspection of the roughness, cleanliness and wickability of the target surface, the surface where the stains are located; (2) the selection of a sufficient and tractable number of stains out of many (sometimes more than 10,000 [5]) blood stains at the target surface; (3) the measurement of size, shape and orientation of those stains; (4) the inference of impact conditions based on measurements in (3); and (5) the backward reconstruction of drop trajectories compatible with the stains and impact conditions; and (6) the identification of a region of origin in 3D space. Current trajectory reconstruction methods [6] are called the method of strings or the tangent method, and assume that blood drops travel in straight trajectories from the area of origin to the target surface. Software based on same method and assumptions is available and used in crime scenes [7,8].

* Corresponding author.
E-mail address: attinger@iastate.edu (D. Attinger).

https://doi.org/10.1016/j.forsciint.2019.02.003
0379-0738/

It is commonly understood that the assumption of straight trajectories is not expected to induce systematic errors in the determination of the region of convergence, which we define as in [9,10], as the projection of the region of origin on a horizontal surface (e.g. the floor). Some analysts determine the region of convergence in the plane of the spatter pattern, which can be of any orientation, but like the two well-cited works above, we use a horizontal plane where the projections of the trajectories are not affected by gravity. Certainly, methods neglecting gravity and drag forces cause systematic errors in the height determination of the region of origin [11,12]. For instance, [13] showed experimentally that doing so "over-estimates the point of origin and the error associated with this technique is significant (50% on average)." Such error is significant enough to wrongly conclude that a person was standing when in fact they may have been sitting. The magnitude of this error is difficult to estimate, because it arises from the use of a physically inconsistent model. It has been conjectured in [14] that "a satisfactory reconstruction" is achieved using straight trajectories if the region of origin is determined "within the volume of a grapefruit, or even a basketball", but there is no universally accepted method to determine the uncertainty associated with the method of strings.

Here, we focus on the common situation where the spatter pattern is found on a vertical wall, as depicted in Fig. 1. A description of the method of strings for stains on a vertical wall is given by Carter [9].

Recently, a probabilistic approach has been proposed by Camana [10] to determine the region of convergence. The method relies on the propagation of measurement uncertainties to the horizontal projections of the trajectories, and constructs a joint probability density function describing the probability that convergence would be within a given spatial region. Of interest is that the method generates a probabilistic map for the area of convergence, directly linking the angles of impact and their uncertainties, to the region of convergence and its area. In other words, [10] proposes for the first time a rational method to estimate the magnitude of the uncertainty around the most likely point of convergence. The ability to rationally provide the uncertainty of a measurement is an important component in expert testimony.

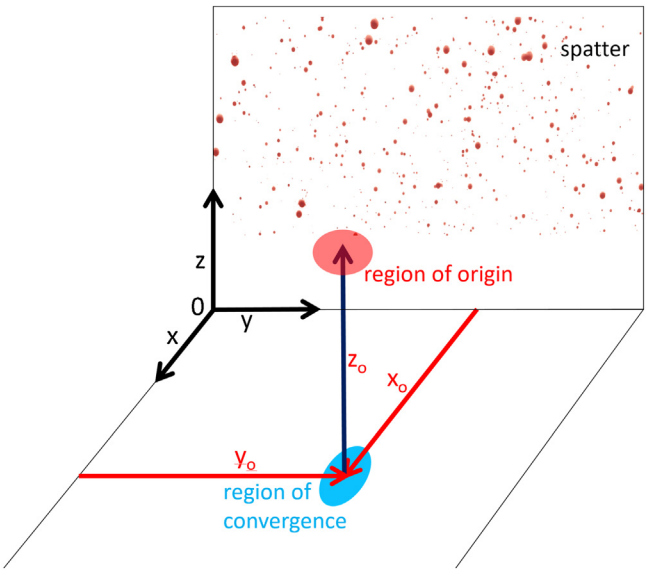

Fig. 1. The problem at hand is the determination of the region of origin of a blood spatter pattern on a vertical wall. The coordinate system used in this manuscript is mentioned, with subscript "o" indicating the origin of the blood, and "0" being the origin of the coordinate trihedron. Indicated are the region of origin – the location where the blood was atomized – and its projection on a horizontal plane, the region of convergence.

In parallel, several approaches have been proposed to consider the effects of drag and gravity on the backward trajectories in BPA. Buck et al. [15] reconstructed drop trajectories with a modified ballistic model, considering gravity and drag forces. In their ballistic analysis, they screened a range of velocity values for compatibility with the preservation of the drop during the flight, since higher velocities result in drop breakup when drag forces overcome the surface tension. While an incorrect assumption on the fluid dynamics of drop impact associated with their analysis is discussed in [16], the present work is inspired by their work. A statistical procedure [17] based on aggregate statistics and basic equations of projectile motion has been shown to determine the region of origin of a blood spatter pattern for cases when the spatter is launched within a narrow range of polar angles — which is the case in, e.g. arterial gushing, but not in beatings or shootings [18]. Attinger et al. [11] proposed a method to reconstruct the ballistic trajectory of a blood drop considering gravity and drag forces. By measuring the volume and shape of the bloodstain on the substrate, the diameter and the velocity of the original drop could be estimated. Such a method was implemented in [19,20], independently. While theoretically portable to crimes scenes, that approach is of limited use, because it requires a high-resolution 3D scanning of bloodstains, surfaces which are both non-absorbing and with roughness significantly smaller than typical stain thickness (10–100 μm). Also, stains are assumed not to contain internal voids, an assumption that is not always correct [4]. Very recently, Comiskey et al. [21] proposed a method to predict trajectories resulting from gunshot spatter patterns, accounting for the effect of air entrainment in the cloud of atomized drops and the aerodynamic drop-drop interaction. While the latter effect might be important near the origin, it is not clear at this time how this time-forward method can be used to reconstruct trajectories backward in time.

In this manuscript, we extend the probabilistic approach of Camana [10], aimed at finding the region of convergence of a blood spatter pattern in a 2D space, to the determination of the region of origin in a 3D space. The core idea of the proposed method is as follows: for each stain of interest, impact angles are estimated from the orientation and ellipticity of the stain. Then, fluid dynamics arguments determine a finite range of possible impact conditions (as proposed in [15]) in terms of pairs of drop diameters and velocities, which correspond to a finite range of possible backward trajectories. Those fluid dynamics arguments consider drop deformation and breakup during flight and impact, the latter being visible by inspection of the periphery of the stain. Then, we statistically identify a 3D region from which the physically sound trajectories most probably originate. That region is called the region of origin, and defined not as a point but as a series of nested volumes. Those volumes can be represented as a set of Russian dolls, the smaller internal ones corresponding to a region of origin determined with a lower probability than the larger ones. Analogous to [10], the proposed method propagates measurement uncertainties and determines the volume of the region of origin based on fluid dynamics and statistics, for the spatter pattern of interest.

Hereafter, we describe the method mathematically, and apply it to published blood spatter pattern data [5] on vertical walls.

2. Methods

2.1. Blood preparation and other experimental details

The blood preparation and experimental methods are described in detail in the published, open-source data set [5] of impact blood spatter patterns and are only briefly discussed here. Namely, blood spatter patterns were generated by impact of either a

cylindrical or a flat surface on a ~1 mL pool of blood resting on another flat surface. Such processes generate spatter patterns similar to those generated during beating incidents or when stepping in puddles of blood. Spatter patterns were produced on vertical targets consisting of assembled flat vertical cardstock sheets with a total area up to 1.5 m^2. The target was placed on the front wall (x = 0) of a room where the air was quiescent. The geometry and coordinate system of the experiment are illustrated in Fig. 1.

The blood was less than two days old, from healthy swine, and gently rocked before the experiment. The temperature, anticoagulant and hematocrit are mentioned in [5]. The generated spatter patterns were scanned at a high resolution of 600 DPI. In comparison with photography with a high-end camera, scanning offers a higher resolution and suppresses parallax error.

A wide range of horizontal distances (x_o = 30 cm to 190 cm) were considered between the target and the blood source. The other parameter that varied during the experiments was the speed of impact (2–9 m/s). Possibly, spatter patterns generated with a larger amount of blood, or with different mechanisms such as gunshot, a rat trap or a shoe step, would have resulted in different size distributions and spatial distributions of stains.

2.2. Trajectory reconstruction process

The method described in this paper is based on fluid dynamics and probability theory. The following sections describe the physical and probabilistic modeling involved in the proposed method, and its implementation.

2.2.1. Fluid Dynamics

There is a wide body of engineering literature describing the trajectories of flying drops, in relation to, e.g., inkjet printing [11], fuel injection [22], or raindrops [23]. The trajectories of flying drops are described with an equation of motion based on Newton's law:

$$m_d \frac{d\vec{V}}{dt} = m_d \vec{g} - \vec{F_D}. \quad (1)$$

Above, m_d, t, $\vec{V}$, $\vec{g}$, $\vec{F_D}$ are the drop mass, time, drop velocity, gravity acceleration and drag force, respectively. It is assumed that the air is quiescent, and that the interactions between drops are negligible. Lift forces are also neglected — those would matter if the drop spins and such information is unavailable at the time of reconstruction.

To calculate the equation of motion (1), it is necessary to estimate the drag caused by the air on the travelling droplet. The drag force is defined as in [11],

$$\vec{F_D} = \rho_a C_D \frac{A_d}{2} \vec{V} V, \quad (2)$$

where ρ_a, A_d, V and $\vec{V}$ are the air density, the cross-sectional area of the undeformed droplet ($A_d = \pi D^2/4$), the velocity magnitude, and velocity vector of the droplet, respectively. The dimensionless parameter C_D is a drag coefficient for an isolated spherical particle, modified to account for the significant particle deformation that occurs at intermediate Weber numbers, as described in the Supplementary documentation.

Determining the region of origin implies backward trajectory reconstruction using Eq. (1). To do so, it is necessary to determine the impact conditions, which are the drop size D, and the impact velocity [11]. The impact velocity can be expressed with three orthogonal velocity components $\vec{V} = \begin{pmatrix} u \\ v \\ w \end{pmatrix}$, or (as done here) with a scalar measure of the velocity magnitude and two angles defining its direction. The scalar measure is either the magnitude of the velocity vector, V, or that of its component normal to the wall, u. The two angles are the directional angle γ, measured clockwise from a vertical line to the major axis of an ellipse fitted on the bloodstain, and the impact angle which is estimated as,

$$\alpha \cong arcsin(W/L), \quad (3)$$

with L and W the respective length and width of an ellipse fitted to the stain.

To determine the remaining impact conditions, we first note that for any given stain, the impact velocity is not independent of the drop diameter. Indeed, a relation between normal impact velocity, u and drop diameter, D can be established from a fluid dynamic correlation between the amount of spreading of a drop into a stain and its impact conditions. Based on dimensional analysis, the above relation can be expressed [24] in the way proposed by Bousfield and Scheller [25,26],

$$\beta = W/D = a\left(Re_N^2 Oh\right)^b \quad (4)$$

Above, β is the spread factor expressing how much the drop spreads upon impact. It is defined as the ratio of stain width over drop diameter. The coefficients are specific to the impact surface, for the cardstock used in this study, a = 0.257 and b = 0.235 [27]; the Reynolds number, $Re_N = \rho u D/\mu$, measures the ratio of the blood inertia normal to the impact surface to the viscous forces inside the drop, and the Ohnesorge number, $Oh = \mu/\sqrt{\rho D \sigma}$, scales the viscous and surface tension forces. Symbols ρ,μ, and σ are the density, viscosity, and surface tension of the blood drop, respectively, and u is the velocity component normal to the target. The above Correlation (4), can be rewritten to express the velocity, u, as an explicit function of drop diameter, D, for a given β, as,

$$u = \frac{\left(\frac{\beta}{a}\right)^{\frac{1}{2b}} \sqrt{\mu\sqrt{\sigma}}}{(\rho D)^{3/4}}. \quad (5)$$

Typically, the spread factor β is within a range of 1.25–6, which corresponds to impacts with very large and very low deformations reviewed in the literature [28]. For any given stain, any trial value β_{trial} within the above range is compatible with the fluid dynamics of the impact; together with the measured stain size and impact angle, β_{trial} corresponds to a trial impact velocity u of a droplet and a trial diameter D by Eqs. (4) and (5), respectively. Thus, for any measured stain, β_{trial} determines a possible impact condition (D_{trial}, u_{trial}, α, γ), so that a trial trajectory can be calculated by integrating the equation of motion (Eq. (1)) backward in time.

Note that the above approach assumes that a set of trial trajectories is issued from each stain, in the manner of [15], and that this set is determined by the range of possible trial values of the spread factor. A first step to reduce the uncertainty on the region of origin is therefore to restrict the possible range of values of the spread factor. Two physical criteria are applied to do so, effectively eliminating non-physical trajectories:

1) Flight breakup criterion: flying drops can break-up when the aerodynamic drag forces acting on the drop exceed the cohesive surface tension forces. A measure of the ratio of the inertial forces to the surface tension forces is the Weber number based on the density of the air ρ_a. Thus the condition that no break-up occurs along the trajectory is expressed as,

$$We_a = \frac{\rho_a D V^2}{\sigma} < K, \quad (6)$$

where V is the maximum velocity along the trajectory from the stain to the region above the area of convergence. The critical Weber number K for drop breakup in flight is set to 13, consistently with extensive experimental studies by Hsiang and

Faeth [29]. This criterion serves as an upper bound for the allowable velocity of a trial trajectory.

2) Stain shape criterion: a second criterion is based on the stain periphery being compatible with the deformation occurring of the moving drop upon impact on a rigid target. It has been shown that upon normal impact [30] when inertial forces are negligible with respect to surface tension forces, the periphery of a blood stain is a smooth circle. For impacts with higher inertia, of magnitude comparable to surface tension, the periphery of the stain exhibits deformation such as waves or spines. Further increase of impact inertia induces splashing [31], visible in [30], where tiny "splashed" stains surround the leading edge of the main stain. This morphological transition, from smooth to wavy to splashed stain boundary, was already observed in 1939 [4] for normal and oblique impacts. While its use for trajectory reconstruction was considered at the time, it has never been successfully implemented, probably because of the abundance of parameters influencing the transition (angle of impact, impact velocity, drop size, substrate roughness). Recently, Bird et al. [32] described the related transition from smooth drop boundary to splashing for the more complex case of oblique impact, in a phase diagram with axes defined in terms of only two dimensionless impact numbers. The description of physical transitions with dimensionless numbers is typical of fluid dynamics, and allows one to describe a phenomenon, here the shape transition at the edge of drops occurring upon impact, with less variables. This reduction of the number of variables thus transforms the intractable problem identified in [4] into a tractable one.

The first dimensionless number, $We_n Re_n^{1/2}$, can be considered as a measure of the ratio of inertial forces – which drive the impact, over the viscous and surface tension forces – which resist the impact. The second dimensionless number, $V_t/V_n\sqrt{Re_n}$, is the ratio of the tangential impact velocity over the normal impact velocity, scaled by the Reynolds number term. It accounts for the effect of angular impact, which typically enhances the tendency to splash at the leading edge of the droplet, and reduces it at its trailing edge. Indeed, experiments done for this work, using the blood and target material of interest, show that the two dimensionless numbers of [32] can be used to associate blood stain shapes with impact conditions, as in the phase diagram of Fig. 2. That figure exhibits insets with typical stain shapes, and calibration performed in this study (described in Supplementary documentation) identified the limits between the three stain peripheral shapes with red and green lines. Above the red line, inertia dominates the resisting forces, and stains exhibit splashing in the form of smaller satellite spatter stains surrounding the leading edge of the main stain, as shown in the insets. Below the green line, inertia is lowest with respect to resisting forces, and stains exhibit a smooth boundary, symmetrical across their main axis. Between the red and the green line, stains exhibit wavy, asymmetric deformations of their boundaries. Note that a typical calibration process such as the one performed in this study for smooth cardstock can be done for other surfaces of interest to crime scene reconstruction. The calibration process provides both the phase diagram in Fig. 2 and the spreading Correlation (4) for a specific target surface.

For the model presented in this manuscript, the phase diagram of Fig. 2 is used to narrow down the range of acceptable trial values of β. Trial impact conditions that correspond to a stain periphery shape different from that observed on the stain of interest are discarded.

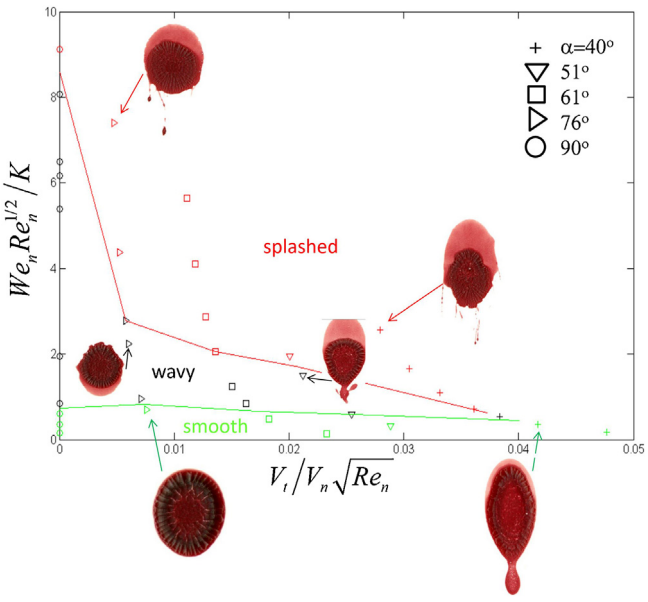

Fig. 2. Phase diagram linking three different morphologies of stain boundaries (smooth, wavy, and splashed) to the impact conditions in terms of dimensionless numbers. Each symbol on the plot corresponds to a measurement of at least 10 drops. The color of the symbol identifies the shape corresponding to the majority of the stains of a given calibration measurement (splashed, wavy or smooth).

Effectively, consideration of this criterion linking the morphology of stain boundary with impact conditions reduces the range of impact conditions to be used in trial trajectory calculations.

2.2.2. Probabilistic modeling

The probabilistic determination of the region of origin is based on the principle of maximum likelihood [33], which identifies the region of origin around a point of highest probability given our assumptions. The likelihood function is then used to produce the region of origin as a confidence volume around that point with varying levels of probability. Fig. 3 describes the method graphically, where the likely region of convergence is first determined in the probabilistic manner of [10], and then the likely height above the region of convergence is estimated. To first determine the region of convergence, the horizontal plane is discretized along its x–y orthonormal directions with an array of points k, as in Fig. 3. A probability density function (PDF) ψ_{ik} expresses the probability density that the x–y projection of a trajectory from stain i passes through point k. As in [10], the PDF is

$$\psi_{ik} = \frac{1}{\Delta\theta_i\sqrt{2\pi}}\exp\left(-\frac{\theta_{ik}^2}{2\Delta\theta_i^2}\right), \tag{7}$$

where θ_{ik} is the angle between the wall and the horizontal projection of the segment between stain i and point k. The direction of the x–y projection of the trajectory towards stain i is determined as,

$$\theta_i = \frac{\pi}{2} + \arctan\left(-\frac{\sin(\gamma_i)}{\tan(\alpha_i)}\right). \tag{8}$$

The uncertainty $\Delta\theta_i$ (1/2 standard deviation) is determined using the propagation of uncertainties, where E is the absolute error in measuring the length L or width W of a stain as in [10],

$$\Delta\theta_i = \sqrt{\frac{L^4\sin^2\gamma}{(L^2-W^2)\cdot[\sin^2\gamma(L^2-W^2)+W^2]}\cdot\left[\frac{W^2}{L^2}E^2 + E^2 + \frac{W^2\cos^2\gamma}{L^4\sin^2\gamma}(L^2-W^2)^2(\partial\gamma)^2\right]}. \tag{9}$$

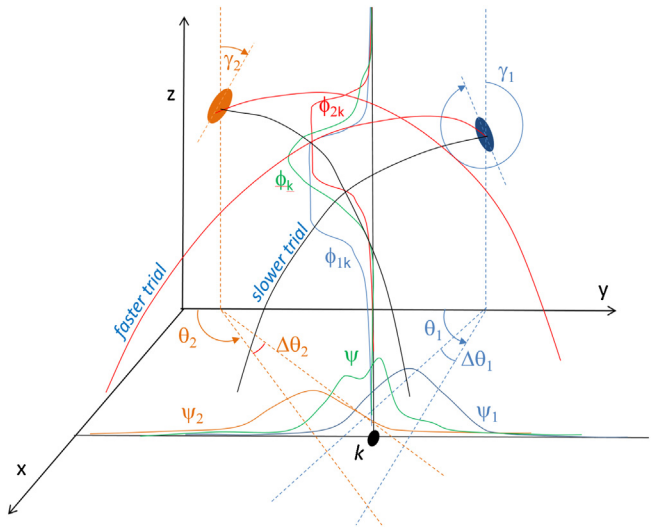

Fig. 3. A probabilistic method to evaluate the region of origin of a blood spatter pattern. Here, two stains $i = 1,2$ are illustrated in blue and orange, respectively, but the method is compatible with large numbers of stains. From each stain, a range of trial trajectories are reconstructed. Fluid dynamic principles guide the reconstruction and the range of trial trajectories (the faster trajectory in red, and the slower, in black). The directional angle γ is measured by stain inspection, and θ_i is the direction of the drop trajectories projected on a horizontal plane. On the horizontal plane, the likelihood ψ determines the location of the region of convergence, and is obtained as a product of the probability density functions (PDFs) of each stain ψ_i. On the vertical axis, the likelihood ϕ_k determines the height of the origin above point k of the region of convergence, and is obtained as a product of the PDFs of each stain ϕ_{ik}. The region of origin is then constructed as a product of ψ and ϕ. (For interpretation of the references to color in this figure legend and text, the reader is referred to the web version of this article.)

Above, the uncertainty on the measurement of the directional angle γ (expressed in radians) is estimated from repeated measurements as $\partial\gamma = 0.07\exp(3.1\alpha)$. The above expression assumes that the measurements of W, L and E are independent, and is valid for $(|\gamma| \in]0, \pi[)$ and $L > W$. Simpler expressions for the limit cases, $\gamma = \pi/2$, or, $\gamma = 0$, are in [10] and [34].

The second PDF, ϕ_{ik}, describes the probability density that the trajectory from stain i passes at a height z above point k. Because there is no known criterion to prefer any trajectory among the ones compatible with the two criterion of flight breakup and stain shape, we assign equal probability to any of those compatible trajectories, using a uniform distribution. This uniform distribution is shown below with Gaussian tails added to account for trajectories with conditions narrowly close to the interval of maximum probability and for the sake of numerical stability in the maximum likelihood estimation as

$$\phi_{ik}(z) = \begin{cases} A, & z_{\min} \le z \le z_{\max} \\ \dfrac{A}{\Delta z}\exp\left[-\dfrac{1}{2}\left(\dfrac{z_{\min}-z}{\Delta z}\right)^2\right], & z < z_{\min}, \\ \dfrac{A}{\Delta z}\exp\left[-\dfrac{1}{2}\left(\dfrac{z-z_{\max}}{\Delta z}\right)^2\right], & z > z_{\max} \end{cases} \quad (10)$$

where A is a normalization constant, and $\Delta z = z_{\max} - z_{\min}$ is the difference between the height of the highest and lowest trajectories compatible with the flight and stain shape criteria, aimed at stain i above point k.

For N stains selected out of a blood spatter pattern, we can calculate the likelihood ψ_k that their trajectories transit above a given point k on the floor as,

$$\psi_k = \prod_{i=1}^{N} \psi_{ik}, \quad (11)$$

and the likelihood $\phi_k(z)$ that their trajectories pass at a given height z over point k as,

$$\phi_k(z) = \prod_{i=1}^{N} \phi_{ik}(z). \quad (12)$$

Note that both definitions above assume that impact processes i are independent from each other. In other words, each stain forms independently from one another.

Then, the probability density function, f, that a blood spatter pattern originates from a given location in 3D space (k, z), where k refers to a position in the horizontal plane, is defined as,

$$f(k,z) = B\psi_k \cdot \phi_k(z). \quad (13)$$

Using a normalization constant, B, the spatial location maximizing f corresponds to the maximum likelihood of the trajectories passing by that location. The probability that the region of origin is within a given volume Ω can be expressed as,

$$P = \int_{\Omega} f(k,z)d\Omega. \quad (14)$$

Fig. 3 illustrates this method for the case where N = 2 stains.

To summarize, the main idea of the method is to first determine the region of convergence in a horizontal plane as the area most compatible with projected trajectories (which are straight lines), and then for every discretized point of the area of convergence, to determine the range of height compatible with physical trajectories.

2.2.3. Implementation

Eight available digital spatter patterns scanned at high resolution, and publicly available [5] are used as input for the simulations. Their names, distance to the wall and velocity of the impactor are in Table 1.

The reconstruction model presented in this manuscript is implemented in the scientific computing language MATLAB [35] version 2013b. Stains are automatically segmented (extracted as a geometrical entity from their background), and ellipses are automatically fitted [36]. The equation of motion (1) are integrated with the ordinary differential equation solver 'ode 45'.

Note that per design, the angles γ and α measured on a stain, i, define the natural direction θ_i of the horizontal projection of the trajectory, within the uncertainty $\Delta\theta_i$. To calculate trajectories with horizontal projections in the vicinity of the projection of that natural trajectory, it is necessary to perturb the trial impact velocity, according to a procedure described in the supplementary documentation.

Table 1
Description of the spatter patterns used in this study, representing a range of impact conditions. Name refers to [5], which provides high-resolution pictures and experimental details of each spatter pattern.

Name	Distance blood source to target wall, x_0, cm	Velocity of impactor, m/s	Type of impact
C9 (slow impact, blood source far from the wall)	120	2.4	Two flat surfaces colliding
HP 31 (fast impact, blood source close to wall)	30	7.8	Rod hitting flat surface
HP 7	60	5.2	
HP 53	60	7.8	
HP 30	60	7.8	
HP 11	120	5.2	
HP 24	120	7.8	
HP 21	190	7.8	

For each spatter pattern, a set of about 40 stains were automatically and randomly selected for reconstruction purposes. The criteria for stain selection were: (1) stains located at least at a given horizontal distance (8% of the horizontal distance between blood source and target) from the centroid of the spatter pattern; (2) stains with ellipticity corresponding to an impact angle between 40° and 75°, corresponding to the available calibration data described in Supplementary documentation; (3) stains that minimize the uncertainty on the angle θ_i as per Eqs. (9) and (4) half the stains with splashing features, and half without, in an attempt to use information from a variety of regions in the phase diagram of Fig. 2. Manual supervision together with automatic comparison of the stain shape with an ellipse were then used to eliminate stains with shapes far remote from ellipses, as it sometimes occurs when multiple stains impact on top of each other, or stains with satellite features that could not be clearly attributed to the stain considered or to neighboring stains. Pictures of selected stains are saved, to preserve the possibility to compare the method at hand with other bloodstain pattern analysis software such as e.g. Hemospat [8]. All the spatter patterns used in this work are available in an open-access dataset [5], in high-resolution, so that other methods of reconstruction or stain selection can be compared with the one presented here.

3. Results and discussion

Reconstruction results are shown and discussed in this section in the following order: (1) reconstruction results of two spatter patterns representing a wide range of conditions: fast impact close to the wall for Fig. 4 and slow impact far from the wall for Fig. 5; (2)

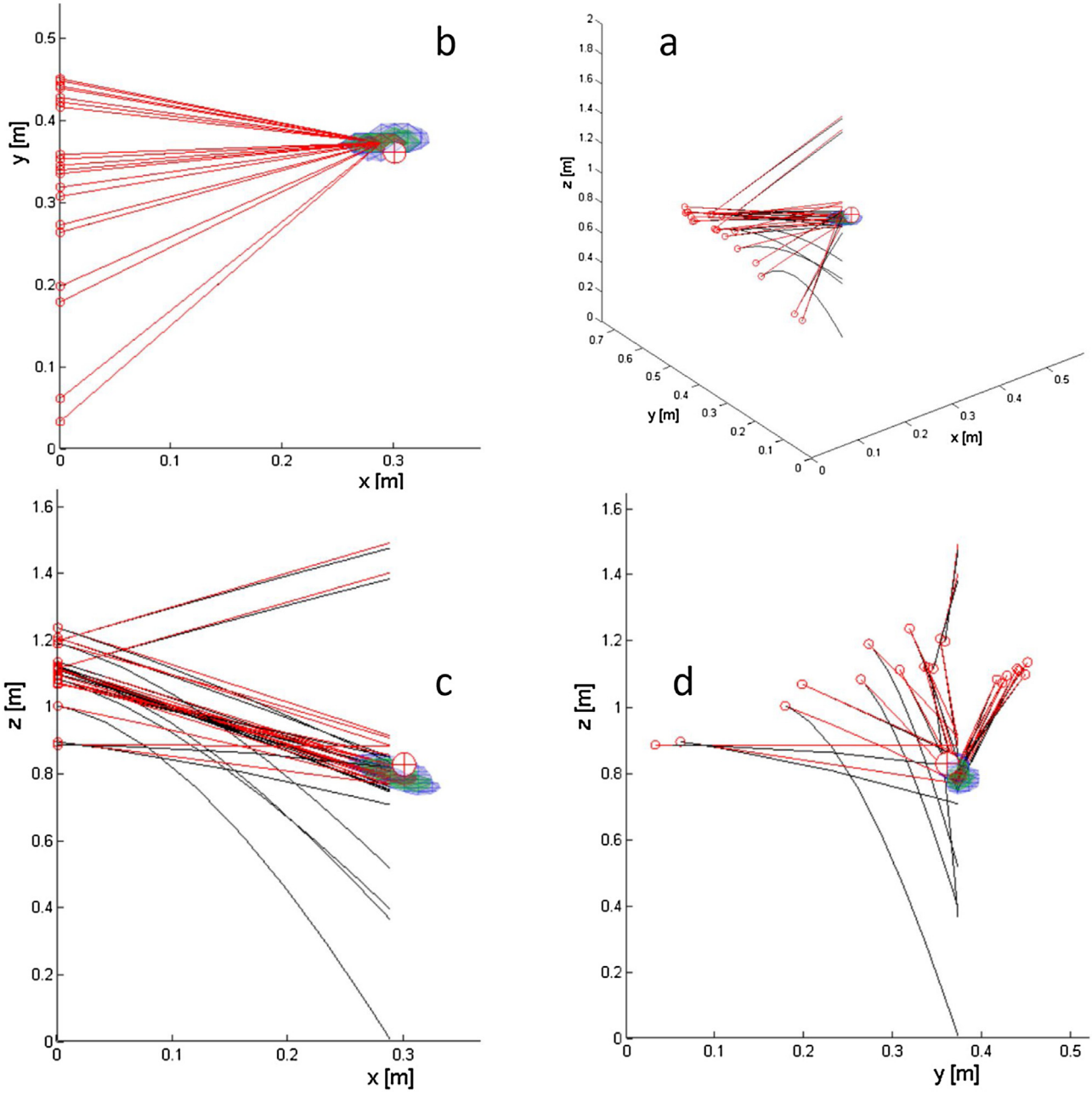

Fig. 4. Reconstruction of trajectories for spatter pattern HP 31, corresponding to a fast impact, close from the wall (x_o = 30 cm). 3D view (a), top view (b), side view (c), and view from the stained wall (d) of the trajectories and the region of origin. The region of origin is represented as concentric volumes, where red, green and blue colors correspond to probability values P of 90%, 99% and 99.9%, respectively. Trajectories with the highest energy are in red, and trajectories with the lowest energy are in black. The known origin is shown by a white disk with a red cross. (For interpretation of the references to color in this figure legend and text, the reader is referred to the web version of this article.)

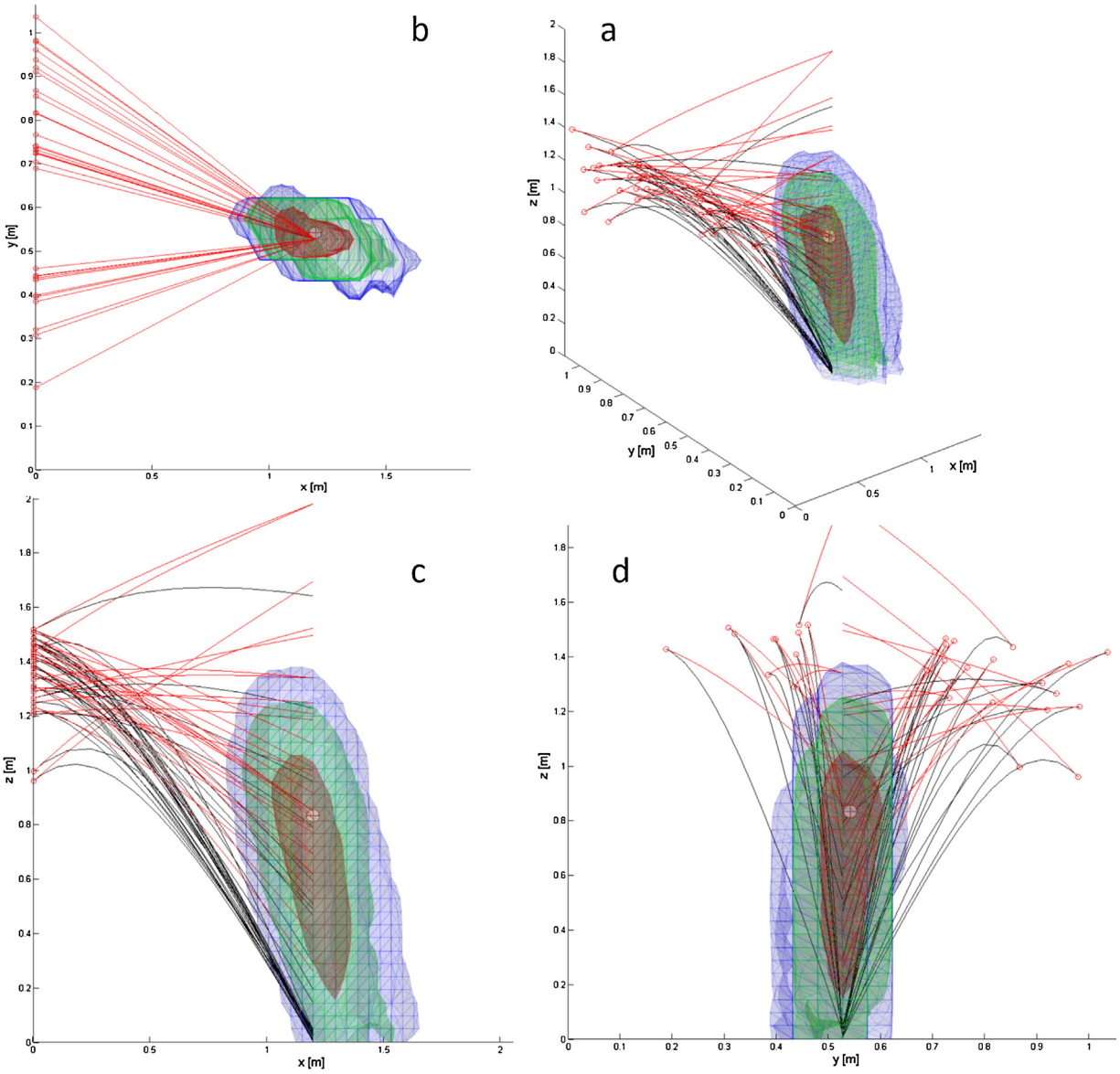

Fig. 5. Results for spatter pattern C9, corresponding to a slow impact, far from the wall (x_o = 120 cm). Axes and colors are the same as in Fig. 4.

uncertainty and error associated with the eight spatter patterns in Table 1, and comparison with state of the art; (3) discussion of the implications for crime scene documentation.

Fig. 4describes views of the reconstruction results for spatter pattern HP 31, corresponding to a fast impact close to the wall, with symbols explained in the figure caption. Trajectories for each stains have been calculated backward, and are plotted between the impact location (x = 0 m) and the location of the known blood source shown as a red cross in a white disk (x_o, y_o, z_o). The trajectories in red are almost straight, because they correspond to the highest impact energy compatible with the stain shape and size. The black trajectories are visibly curved, and correspond to the lowest impact energy compatible with the stain shape and size. The volume of the region of origin can be calculated according to Eq. (14). For a probability P = 99.9%, the region of origin has a volume of 0.11 L, which is about a tenth of that of a grapefruit, a commonly used estimate of the volume of the region of origin. Note that some stains pointing downwards are also considered in the reconstruction.

Reconstruction results for an impact slower with an origin far away from the wall, are in Fig. 5. The volume of the region of origin increases drastically. Here the region of origin has a volume of 95 L, which correspond to about 93 grapefruits or 13 basketballs — another proposed estimate of the volume of the region of origin [14]. Interestingly, the major uncertainty is along the vertical axis. Similarly to the previous result, some stains pointing downwards are also considered in the reconstruction.

Similar reconstruction efforts have been undertaken with the six other spatter patterns referenced in Table 1. The volume of the region of origin, which corresponds to the uncertainty in the determination of the origin, is plotted in Fig. 6 using Eq. (14), with the values of the PDF that correspond to blue, green or red region of origin in Fig. 5. Fig. 6 reveals that the uncertainty V_{RO} is proportional to the distance x_0 between source and wall at a power of about five,

$$V_{RO} \sim x_O^n, \text{ with } 5.2 \leq n \leq 5.5. \quad (15)$$

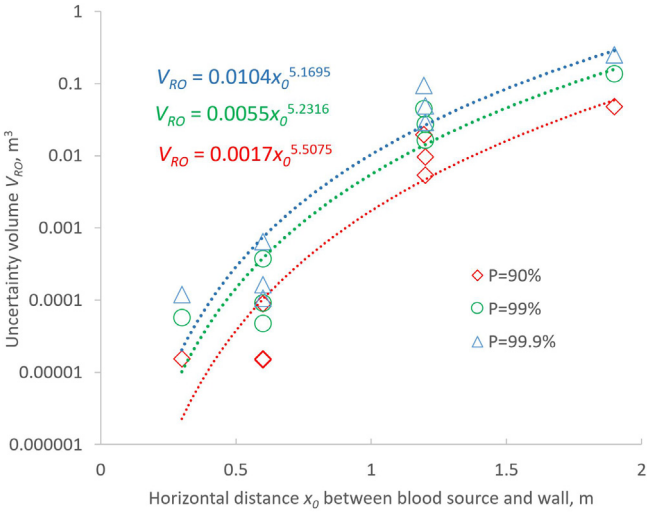

Fig. 6. Volume of the region of origin as a function of the horizontal distance between blood source and wall, as determined by the reconstruction method presented in this manuscript. Parameter P is the value of the probability value used to define the region of origin, Eq. (14).

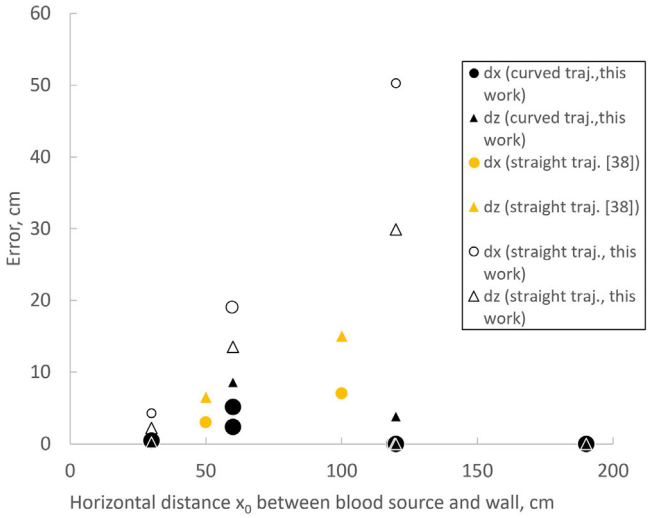

Fig. 7. Error in the determination of the region of origin as a function of the horizontal distance between blood source and wall, as determined by the reconstruction method presented in this manuscript. For comparison, results using reconstruction methods assuming straight trajectories are also plotted.

The above estimate confirms that the volume of the region of origin has a strong dependence on the distance from the wall. This value can be explained because the uncertainty in either horizontal direction grows linearly with the distance x_O as $\Delta x \approx x_o$, and $\Delta y \approx x_o$, while the uncertainty in the vertical direction grows as $\Delta z \approx gt^2/2$. Assuming a steady horizontal velocity u of the drop, the travel time $t \approx x_O/u$. Combining the two latter assumptions results in $\Delta z \approx g x_0^2/(2u^2)$. Thus a rough estimate of the uncertainty $V_{RO} \cong \Delta x \cdot \Delta y \cdot \Delta z \approx x_0^4$. Numerically, the exponent of the power law in Eq. (15) is about five. Also, the assumption of Δz is inversely proportional to the square of the velocity, which indicates that selecting stains generated from faster drops might decrease reconstruction uncertainty. Note that in both spatter patterns reconstructed in the above figures, some stains pointing downwards are considered, while these are typically excluded from height reconstruction using traditional reconstruction methods.

Besides the uncertainty on the determination of the region of origin, we can also determine its error. The error in the determination of the region of origin is defined in the classical manner [37] as the difference between the estimated and the known region of origin of a spatter pattern. Here, it is calculated as the smallest vector between the determined region of origin and the known region of origin. Fig. 7 plots the absolute values of the horizontal (dx) and vertical (dz) components of this error, assuming a probability $P = 99\%$, as a function of the horizontal distance between blood source and wall. Typically, dx is negative (the source is found closer to the wall), and dz is positive (the source is found higher than it actual location). The error of the present method, at least with the eight spatter patterns studied, is always smaller than 10 cm, and does not grow with the distance from the wall. Although typically negligible in a crime scene, and independent of the distance from the wall, the error is not always zero. This means that with the present method, the known region of origin is not always within the determined region of origin. Possible reasons for this are: the assumption that ellipticity exactly determines the impact angle (Eq. (3)), no matter the stain size or impact energy; the equations of motion (Eq. (1)) that neglects interactions between drops; the drag coefficient that neglects oscillations of drops, while considering their steady deformation; and the fact that atomization occurs over a volume rather than a specific point. From the eight spatter patterns examined, it appears that the present method does not exhibit a systematic bias or error. A comparison is made with a systematic study [38] on the sources of error in reconstruction using straight trajectories. Since no peer-reviewed results could be found for spatter patterns more than one meter away from the wall, additional reconstruction results assuming straight trajectories obtained by participants to a workshop given by the first author are also plotted in green. The data points obtained while assuming straight trajectories (in yellow and green) are averaged from several trials. In comparison, the method of strings shows a systematic error in the determination of the height: the determined height is higher than the known height. This bias is well known by BPA researchers and practitioners [6,39]. Another contribution of the present method is to estimate the uncertainty associated with the reconstruction of a specific spatter pattern.

Should the above method be used on a crime scene, two recommendations for crime scene documentation should be stated. Since the method relies on inspection of the stain boundaries, it is important to photograph stains with the highest possible resolution. In this study, a resolution of 600 dots per inch was used. Using a macro-lens and a state-of-the-art digital camera, resolutions of the same order can been reached by stitching [40] multiple images of small areas ($O(10\,\text{cm} \times 10\,\text{cm})$). Protocols for reliable stitching and for quality illumination in the macro-photography process – where the camera objective is close to the object – would have to be designed. Also, the transitions between stain shapes depend on the blood and target material on which stains are found, which has implications in documentation and preservation of evidence. Until reliable calibration data is provided, we recommend that investigators collect samples of the target surface of interest and hematocrit measurements. Note also that in a real crime scene, it is not uncommon that the blood source moves during the generation of the blood spatter. That fact will add additional uncertainty in the determination of the region of origin.

4. Conclusion

In this study, we propose a novel method based on sound fluid dynamics and a probabilistic approach to determine the region of origin of the impact blood spatter patterns associated with

beatings. The method is based on the inspection of high-resolution images of the spatter patterns, where the presence or absence of splashing traces at the periphery of drops is used to narrow down the possible range of impact conditions. A range of spatter patterns with various impact energies and distances between the source and spatter pattern is reconstructed with the proposed method. The region of origin of a blood spatter pattern is quantified in the form of a volume surrounding the most likely point of origin, determined by propagating the uncertainties due to stain measurements. The method presented here allows a rational and case-related estimate of the uncertainty associated with trajectory reconstruction. The statistical framework is flexible and general enough to accommodate current and future advances in the fluid dynamics of blood spatter patterns. Our results suggest that uncertainty grows with a power five of the distance between the spatter pattern and the target, and can reach more than the traditional estimate of the volume of a grapefruit or a basketball. The proposed method allows the consideration of stains pointing downwards. It is the belief of the authors that the proposed reconstruction method can be used to prescribe recommendations on crime scene documentation. Future work will focus on providing calibration data for other target surfaces relevant to crime scenes, and on transitioning this reconstruction method from an academic exercise to a tool useful for crime scene reconstructions.

Acknowledgments

The authors acknowledge financial support from the US National Institute of Justice (Award No. NIJ 2014-DN-BX-K036). This work was also partially funded by the Center for Statistics and Applications in Forensic Evidence (CSAFE) through Cooperative Agreement No. 70NANB15H176 between NIST and Iowa State University, which includes activities carried out at Carnegie Mellon University, University of California Irvine, and University of Virginia. We acknowledge the contribution of Prashant Agrawal, John Polansky and Zaki Jubery in specific aspects of the numerical implementation; useful discussions with Craig Moore; as well as the participants from the Swiss scientific police force to a workshop on the fluid dynamics of BPA in summer 2016 for reconstruction of spatters in Fig. 7.

Appendix A. Supplementary data

Supplementary material related to this article can be found, in the online version, at doi: https://doi.org/10.1016/j.forsciint.2019.02.003.

References

[1] P.L. Kirk, Crime Investigation: physical evidence and the police laboratory, Blood, Physical Investigation, Interscience Publishers, 1953, pp. 176–203.
[2] P.R. De Forest, R.E. Gaensslen, H.C. Lee, Forensic Science: An Introduction to Criminalistics, McGraw-Hill, New York, 1983.
[3] Terms and Definitions in Bloodstain Pattern Analysis, ASB Technical Report 033, first ed., (2017) .
[4] V. Balthazard, R. Piedelievre, H. Desoille, L. Dérobert, Etude des gouttes de sang projeté, XXIIe congrès de médicine légale de langue francaise, (1939) Paris.
[5] D. Attinger, Y. Liu, T. Bybee, K. De Brabanter, A data set of bloodstain patterns for teaching and research in bloodstain pattern analysis: impact beating spatters, Data Brief 18 (2018) 648–654.
[6] T. Bevel, R.M. Gardner, Bloodstain Pattern Analysis with an Introduction to Crime Scene Reconstruction, third ed., CRC Press, Boca Raton, FL, USA, 2008.
[7] A.L. Carter, M. Illes, K. Maloney, A.B. Yamashita, B. Allen, B. Brown, L. Davidson, G. Ellis, J. Gallant, A. Gradkowski, J. Hignell, S. Jory, P.L. Laturnus, C.C. Moore, R. Pembroke, A. Richard, R. Spenard, C. Stewart, Further validation of the BackTrack(TM) computer program for bloodstain pattern analysis: precision and accuracy, Int. Assoc. Bloodstain Pattern Anal. News 21 (3) (2005) 15–22.
[8] K. Maloney, J. Killeen, A. Maloney, The use of HemoSpat to include bloodstains located on nonorthogonal surfaces in area of origin calculations, J. Forensic Identif. 59 (5) (2009) 513.
[9] A.L. Carter, The directional analysis of bloodstain patterns: theory and experimental validation, J. Can. Soc. Forensic Sci. 34 (4) (2001) 173–173.
[10] F. Camana, Determining the area of convergence in Bloodstain Pattern Analysis: A probabilistic approach, Forensic Sci. Int. 1–3 (September (231)) (2013) 131–136.
[11] D. Attinger, C. Moore, A. Donaldson, A. Jafari, H.A. Stone, Fluid dynamics topics in bloodstain pattern analysis: comparative review and research opportunities, Forensic Sci. Int. 231 (1–3) (2013) 375–396 (in English).
[12] Committee on Identifying the Needs of the Forensic Sciences Community, National Research Council (National Research Council), Strengthening Forensic Science in the United States: A Path Forward, The National Academies Press, Washington, DC, 2009. https://doi.org/10.17226/12589.
[13] N. Behrooz, L. Hulse-Smith, S. Chandra, An evaluation of the underlying mechanisms of bloodstain pattern analysis error, J. Forensic Sci. 56 (September (5)) (2011) 1136–1142.
[14] H.L. MacDonell, Bloodstain Patterns, second ed., Laboratory of Forensic Sciences, Corning, NY USA, 2005.
[15] U. Buck, B. Kneubuehl, S. Näther, N. Albertini, L. Schmidt, M. Thali, 3D bloodstain pattern analysis: ballistic reconstruction of the trajectories of blood drops and determination of the centres of origin of the bloodstains (in English), Forensic Sci. Int. 206 (March (1–3)) (2011) 22–28.
[16] P.A. Pizzola, J.M. Buszka, N. Marin, N.D.K. Petraco, P.R. De Forest, Commentary on "3D bloodstain pattern analysis: ballistic reconstruction of the trajectories of blood drops and determination of the centres of origin of the bloodstains" by Buck et al. [Forensic Sci. Int. 206 (2011) 22–28] (in English), Forensic Sci. Int. Lett. 220 (2012) e39–e40.
[17] C.R. Varney, F. Gittes, Locating the source of projectile fluid droplets, Am. J. Phys. 79 (8) (2011) 838–842.
[18] P.M. Comiskey, A.L. Yarin, D. Attinger, High-speed video analysis of forward and backward spattered blood droplets, Forensic Sci. Int. 276 (2017) 134–141.
[19] N. Laan, K.G. de Bruin, D. Slenter, J. Wilhelm, M. Jermy, D. Bonn, Bloodstain pattern analysis: implementation of a fluid dynamic model for position determination of victims, Sci. Rep. 5 (2015) 11461.
[20] D. Attinger, Development of a Science Base and Open Source Software for Bloodstain Pattern Analysis, Final Technical Report 2010-DN-BX-K403, (2016) .
[21] P.M. Comiskey, A.L. Yarin, S. Kim, D. Attinger, Prediction of blood back spatter from a gunshot in bloodstain pattern analysis, Phys. Rev. Fluids 1 (4) (2016) 043201.
[22] G.M. Faeth, L.P. Hsiang, P.K. Wu, Structure and breakup properties of sprays, Int. J. Multiph.Flow 21 (December) (1995) 99–127.
[23] M. Vargas, Drag Coefficient of Water Droplets Approaching the Leading Edge of an Airfoil, 5th AIAA Atmospheric and Space Environments Conference (2013) 1–23, doi:http://dx.doi.org/10.2514/6.2013-3054.
[24] R.P. Sahu, S. Sett, A.L. Yarin, B. Pourdeyhimi, Impact of aqueous suspension drops onto non-wettable porous membranes: hydrodynamic focusing and penetration of nanoparticles, Colloids Surf. A 467 (2015) 31–45.
[25] B.L. Scheller, D.W. Bousfield, Newtonian drop impact with a solid surface, AICHE J. 41 (6) (1995) 1357–1367.
[26] C.D. Adam, Fundamental studies of bloodstain formation and characteristics (in English), Forensic Sci. Int. 219 (2012) 76–87.
[27] S. Kim, Y. Ma, P. Agrawal, D. Attinger, How important is it to consider target properties and hematocrit in bloodstain pattern analysis? Forensic Sci. Int. 266 (2016) 178–184.
[28] M. Pasandideh-Fard, Y.M. Qiao, S. Chandra, J. Mostaghimi, Capillary effects during droplet impact on a solid surface, Phys. Fluids 8 (1996) 650–659.
[29] L.P. Hsiang, G.M. Faeth, Near-limit drop deformation and secondary breakup, Int. J. Multiphase Flow 18 (September (5)) (1992) 635–652.
[30] L. Hulse-Smith, N.Z. Mehdizadeh, S. Chandra, Deducing drop size and impact velocity from circular bloodstains, J. Forensic Sci. 50 (1) (2005) 54–63.
[31] C. Mundo, M. Sommerfeld, C. Tropea, Droplet-wall collisions: experimental studies of the deformation and breakup process, Int. J. Multiphase Flow 21 (1995) 151–173.
[32] J.C. Bird, S.S.H. Tsai, H.A. Stone, Inclined to splash: triggering and inhibiting a splash with tangential velocity, New J. Phys. 11 (6) (2009) 1–11 063017.
[33] J.A. Rice, Mathematical Statistics and Data Analysis, third ed., Brooks/Cole, 2007.
[34] C. Willis, A.K. Piranian, J.R. Donaggio, R.J. Barnett, W.F. Rowe, Errors in the estimation of the distance of fall and angles of impact blood drops (in English), Forensic Sci. Int. 123 (November (1)) (2001) 1–4.
[35] G. Recktenwald, Numerical Methods with Matlab: Implementations and Applications, Prentice-Hall, Upper-Saddle River, NJ, 2000.
[36] P.M. Comiskey, A.L. Yarin, D. Attinger, Hydrodynamics of back spatter by blunt bullet gunshot with a link to bloodstain pattern analysis, Phys. Rev. Fluids 2 (7) (2017) 073906.
[37] E.O. Doebelin, Measurement Systems: Application and Design, McGraw-Hill, 2004.
[38] K.G. de Bruin, R.D. Stoel, J.C.M. Limborgh, Improving the point of origin determination in bloodstain pattern analysis, J. Forensic Sci. 56 (6) (2011) 1476–1482.
[39] S.H. James, P.E. Kish, T.P. Sutton, Principles of Bloodstain Pattern Analysis: Theory and Practice, CRC Press, 2005.
[40] S. Siu, J. Pender, F. Springer, F. Tulleners, W. Ristenpart, Quantitative differentiation of bloodstain patterns resulting from gunshot and blunt force impacts (in English), J. Forensic Sci. (Februry) (2017) 1–14.